HHS Public Access

Author manuscript

Biochem Pharmacol. Author manuscript; available in PMC 2020 October 01.

Published in final edited form as:

Biochem Pharmacol. 2019 October ; 168: 204–213. doi:10.1016/j.bcp.2019.07.007.

Profile of Cortical N-methyl-D-aspartate Receptor Subunit Expression Associates with Inherent Motor Impulsivity in Rats

Brionna D. Davis-Reyes, **Veronica M. Campbell**, **Michelle A. Land**, **Holly L. Chapman**, **Susan J. Stafford**, **Noelle C. Anastasio**

Center for Addiction Research and Department of Pharmacology and Toxicology, University of Texas Medical Branch, Galveston, TX USA

Abstract

Impulsivity is a multifaceted behavioral manifestation with implications in several neuropsychiatric disorders. Glutamate neurotransmission through the N-methyl-D-aspartate receptors (NMDARs) in the medial prefrontal cortex (mPFC), an important brain region in decision-making and goal-directed behaviors, plays a key role in motor impulsivity. We discovered that inherent motor impulsivity predicted responsiveness to D-cycloserine (DCS), a partial NMDAR agonist which prompted the hypothesis that inherent motor impulsivity is associated with the pattern of expression of cortical NMDAR subunits (GluN1, GluN2A, GluN2B), specifically the protein levels and synaptosomal trafficking of the NMDAR subunits. Outbred male Sprague Dawley rats were identified as high (HI) or low (LI) impulsive using the one-choice serial reaction time task. Following phenotypic identification, mPFC synaptosomal protein was extracted from HI and LI rats to assess the expression pattern of the NMDAR subunits. Synaptosomal trafficking and stabilization for the GluN2 subunits were investigated by coimmunoprecipitation for postsynaptic density 95 (PSD95) and synapse associated protein 102 (SAP102). HI rats had lower mPFC GluN1 and GluN2A, but higher GluN2B and pGluN2B synaptosomal protein expression versus LI rats. Further, higher GluN2B:PSD95 and GluN2B:SAP102 protein:protein interactions were detected in HI versus LI rats. Thus, the mPFC NMDAR subunit expression pattern and/or synaptosomal trafficking associates with high inherent motor impulsivity. Increased understanding of the complex regulation of NMDAR balance within the mPFC as it relates to inherent motor impulsivity may lead to a better understanding of risk factors for impulse-control disorders.

Graphical Abstract

Correspondence: Noelle C. Anastasio, Ph.D., Center for Addiction Research, Department of Pharmacology and Toxicology, University of Texas Medical Branch, Galveston, Texas USA 77555-0615, 409-772-9656, ncanasta@utmb.edu.

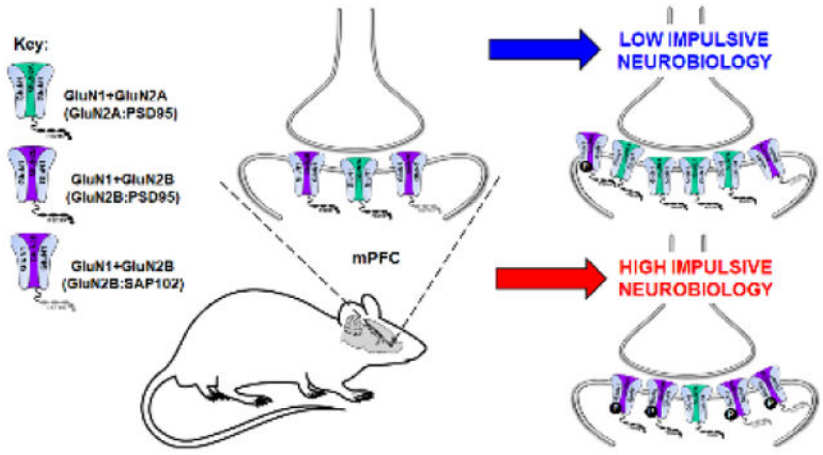

Keywords

Motor impulsivity; medial prefrontal cortex; NMDA receptor; D-cycloserine; MAGUKs

1. Introduction

Impulsivity is a complex multifaceted behavioral construct that is associated with several neuropsychiatric disorders (e.g., attention deficit/hyperactivity disorder, autism, and substance use disorders) [1–3]. It is broadly characterized as behavior without sufficient foresight and has two primary facets—motor impulsivity/impulsive action (difficulty withholding a prepotent motor response) and impulsive choice (preference for small intermediate rewards over large delayed rewards). Impulsivity is reliably assayed with self-report questionnaires in humans [4] and as well as laboratory measures in humans [5–8] and animals [7, 9]. Examining the neurobiological mechanisms underlying individual differences in motor impulsivity represents a unique approach in elucidating impulse-control disorders.

A critical brain region underlying motor impulsive behavior is the medial prefrontal cortex (mPFC), an area integral in executive function and decision making [10] and involved in mediating “stop” signals to reward-associated brain regions [11]. The mPFC is a major hub for glutamatergic output signaling facilitated primarily through the N-methyl-D-aspartate receptor (NMDAR) [12]. The NMDAR is a member of the ionotropic glutamate family of receptors and is composed of multiple subunits, including GluN1 (the obligatory unit) and GluN2A-D, to form a functional heterotetramer [13, 14]. The NMDAR is widely distributed in the mPFC [15], and is activated by binding of glutamate to the GluN2 subunit and the coagonist glycine to the GluN1 subunit [16]. There is also evidence that the spatial distribution (i.e. localization) in the synaptic milieu (for review see [17]), and not solely the subunit composition per se, determines NMDAR-dependent signaling [18]. While NMDAR synaptic localization is incompletely understood, PDZ domain proteins within the postsynaptic density (PSD), a dynamic network of scaffolding proteins and glutamate receptors, mobilizes and localizes NMDARs to the synapse (for review see [19]). The presence or absence of key scaffolding proteins determines the localization of the receptors bound to them. For example, postsynaptic density 95 (PSD95) [20], a member of the

membrane-associated guanylate kinases (MAGUKs) family, binds to receptors and signal transduction proteins to facilitate signaling cascades which plays a fundamental role in the organization of the postsynaptic architecture [21, 22]. PSD95 binds to both GluN2A and GluN2B subunits and tends to stabilize NMDARs to the synapse [23]. Synapse associated protein 102 (SAP102), another member of the MAGUKs family, is linked to NMDAR trafficking [24, 25] and is preferentially associated with GluN2B [26] and regulates GluN2B mobility [27–29]. Further, phosphorylation of specific residues within NMDAR subunits may drive NMDAR trafficking/localization and PDZ protein-protein interactions (for review see [30, 31].

NMDAR antagonism both systemically and intra-mPFC results in an array of behavioral impairments that can be likened to frontal lobe dysfunction [32–35]. Furthermore, glutamate neurotransmission through NMDAR is a critical regulator of impulse-control disorders, for example, antagonism of NMDARs systemically [33, 36–42] or directly in the mPFC [39, 40, 43] elevates impulsivity. Selective antagonism of the GluN2B subunit enhances motor impulsivity [33, 38] and individual differences in impulsive choice determine the effects of NMDAR antagonists [44]. Taken together, these studies suggest that the impulsive phenotype may correspond to differences in cortical NMDAR composition, synaptosomal bioavailability, and association with PDZ proteins.

In the present preclinical study, we aimed to elucidate the role of cortical NMDARs in trait motor impulsivity. To this end, we first employed pharmacological measures via utilization of D-cycloserine (DCS), a partial agonist at the glycine binding site of the NMDAR [45–47]. Second, we employed biochemical measures to assess NMDAR subunit expression and synaptosomal localization in the mPFC. We hypothesized that individual differences in motor impulsivity are driven by the profile of the NMDAR subunits, specifically the expression and localization of the cortical NMDAR subunits as well as the association with PSD95 and SAP102 within the mPFC.

2. Materials and Methods

2.1 Animals

Male, outbred Sprague–Dawley rats (n=215; Envigo, Indianapolis, IN) weighing 250–275g upon arrival were housed two/cage under a 12-h light–dark cycle with controlled temperature (21–23°C) and humidity (40–50%). Animals were acclimated for seven days to the colony room prior to the start of handling and experimental procedures. During the one-choice serial reaction time (1-CSRT) task acquisition and maintenance, rats were food restricted to 90% free-feeding weight; water was available *ad libitum* except during daily operant sessions. Rats were weighed daily to ensure that their body weights were maintained at ~90% of free-feeding levels. All experiments were conducted in accordance with the NIH Guide for the Care and Use of Laboratory Animals (2011) and with the University of Texas Medical Branch Institutional Animal Care and Use Committee approval.

2.2 Drugs

D-cycloserine (DCS) was purchased from Sigma-Aldrich (St. Louis, MO; catalog # C6880–5G) and dissolved in 0.9% NaCl (saline; Baxter Healthcare, Deerfield, IL; catalog # 2F7124).

2.3 Animal Behavior and Pharmacology

2.3.1 1-Choice Serial Reaction Time Task Training—Procedures occurred in standard five-hole nose-poke operant chambers equipped with a house light, food tray, and an external pellet dispenser capable of delivering 45 mg pellets (Bio-Serv, Frenchtown, NJ) housed within ventilated and sound-attenuated chambers (MedAssociates, St Albans, VT). The 1-CSRT task methodology has been described in detail previously [48–53]. Briefly, rats were habituated to the test chamber; a nose-poke into the singly-illuminated center hole resulted in the delivery of one food pellet into the magazine on the opposite wall of the chamber and simultaneous illumination of the magazine light. During this stage, all responses made in the correctly lit (target) hole resulted in the illumination of the magazine light and presentation of a single food pellet. The latency to retrieve the food pellet is recorded. The training stages thereafter were each comprised of daily sessions of 100 trials to be completed in a maximum of 30 min; each training stage involved incrementally lowering the stimulus duration with a 5-sec limited hold and an intertrial interval (ITI) of 5 sec. A maximum of 100 correct responses in a session resulted in a maximum of 100 reinforcers earned; incorrect, premature responses or omissions resulted in a 5-s time-out period and a reduction in reinforcers obtained. Advancement to the next training stage required rats to meet acquisition criteria: ≥50 correct responses, >80% accuracy [correct responses/(correct + incorrect) × 100] and <20% omissions (omitted responses/trials completed × 100). Time to finish the training session is recorded for each rat.

Premature responses [(total premature responses = target premature responses + non-target premature responses; “non-target” indicates premature response detected outside of the center nose poke hole) were employed as the primary indication of motor impulsivity [2, 7, 48–56]. The number of reinforcers earned provides a measure of task competency and a secondary assessment of motor impulsivity, while percent accuracy was a general indication of attentional capacity [2, 7, 48–56]. Percent omissions indicated failures of detection of the visual stimuli in the target hole as well as motivation to perform the task [2, 7, 48–56].

After meeting stability criteria for the final training stage over three consecutive ITI5 sessions (with <20% variability), an ITI8 challenge session was conducted in which the ITI was 8-s for the session [48–53]. Five separate cohorts of outbred rats were trained on the 1-CSRT task and, within each cohort (n=32–46), HI (n=9–15/cohort) and LI (n=8–15/cohort) were stratified as the top and bottom 25% (quartile split) or 33% (tertile split) of rats based upon premature responses on the ITI8 challenge session (Table 1). Quartile and tertile splits were determined based on necessity for tissue for biochemical analyses, and utilization of either stratification method did not change the validity of the phenotypes nor the consistency of the 1-CSRT task output parameters across cohorts (Table 1).

2.3.2 Pharmacological manipulation of motor impulsivity via systemic administration of D-cycloserine—

Rats were trained to criterion on the 1-CRST task and challenged on an ITI8 test session to identify phenotypes. Following ITI8 test session completion, rats were re-stabilized in the 1-CSRT task [≥ 50 target responses, > 80% accuracy, and < 20% omissions on the final training stage (0.5 sec stimulus duration, 5 sec limited hold, and ITI5)] for at least three consecutive days. Performance in the 1-CSRT task was assessed following vehicle (saline, 1 mL/kg; i.p.) or DCS (1, 2, 5, 10, 20, or 50 mg/kg; i.p.;) 15 min prior to the start of 1-CSRT task sessions under ITI5 conditions [Cohort 2 (Fig. 1); Table 1]. Each rat received all doses of DCS in a balanced, pseudo-randomized order. Rats were treated with vehicle the day before DCS treatments and received only one DCS treatment per week.

2.4 Biochemical Assays

2.4.1 Protein Extraction and Capillary Electrophoresis—

Rats were anesthetized (400 mg/kg chloral hydrate solution), decapitated, and brains were cut in 2 mm coronal sections, rapidly microdissected with a scalpel on a cool tray (4°C) [57], frozen in liquid nitrogen and stored at −80°C. Crude synaptosomal protein fraction enriched for pre- and postsynaptic proteins (i.e., presynaptic terminals, postsynaptic membranes, postsynaptic density, synaptic protein complexes) from the mPFC of HI and LI rats [Cohorts 1 (Fig. 2–4) and 3–5 (Figs. 5 and 6); Table 1] was prepared as described previously [1, 48, 49, 58–60]. The crude synaptosomal protein preparation expresses the postsynaptic markers PSD95 and SAP102 (present study, [49, 58], syntaxin (synaptosomal marker) [58], and SNAP25 (presynaptic marker) [58]. Tissue encompassing the mPFC (cingulate cortex 1, prelimbic cortex and infralimbic cortex; 3.00 mm from bregma [61]) was homogenized in 10 times w/v ice cold Krebs buffer (125 mM NaCl, 1.2 mM KCl, 1.2 mM $MgSO_4$, 1.2 mM $CaCl_2$, 22 mM Na_2CO_3, 1 mM NaH_2PO_4, 10 mM glucose) containing 0.32 sucrose plus protease inhibitor cocktail and phosphatase inhibitor 2 and 3 cocktails (10 μL/mL; Sigma-Aldrich, St. Louis, MO). The homogenate was centrifuged at 1000 g for 10 min at 4°C to pellet the nuclear fraction (P1). The supernatant (S1) was collected and centrifuged at 20,000 g for 30 min at 4°C to pellet the crude synaptosome (P2). The pellet was re-suspended in Krebs buffer with 0.5% NP40. All protein fractions were stored at −20°C until use.

Crude synaptosomal protein prepared from the mPFC were subjected to the Wes™ automated western blotting system (ProteinSimple, San Jose, CA), which utilizes capillary electrophoresis-based immunodetection for higher resolution, sensitivity, and reproducibility (even at low sample concentrations) relative to traditional immunoblotting techniques [1, 49, 54, 60]. Wes™ reagents (biotinylated molecular weight marker, streptavidin-HRP fluorescent standards, luminol-S, hydrogen peroxide, sample buffer, DTT, stacking matrix, separation matrix, running buffer, wash buffer, matrix removal buffer, secondary antibodies, antibody diluent, and capillaries) were obtained from the manufacturer (ProteinSimple) and used according to the manufacturer's recommendations with minor modifications [1, 60]. Antibodies targeting GluN1 (1:1000; BD Pharmingen, San Jose, CA; catalog # 556308), GluN2A (1:250; Millipore, Burlington, MA; catalog # AB1555P), GluN2B (1:250; Millipore; catalog # AB1557P), and phosphorylated-GluN2B at Ser1303 (pGluN2B, 1:500; Millipore, catalog # 07–398) were employed. Equal amounts of protein (2 μg) were

combined with 0.1X sample buffer and 5X master mix (200 mM DTT, 5X sample buffer, 5X fluorescent standards), gently mixed, and then denatured at 90°C for 10 min. The denatured samples, biotinylated ladder, antibody diluent, primary antibodies, horseradish peroxidase (HRP) conjugated secondary antibodies, chemiluminescent substrate, and wash buffer were dispensed to designated wells in a pre-filled microplate. Separation electrophoresis (375 V, 28 min, 25°C) and immunodetection in the capillaries were fully automated using the following settings: separation matrix load for 200 sec, stacking matrix load for 20 sec, sample load for 12 sec, antibody diluent for 30 min, primary antibody incubation for 60 min, secondary antibody incubation for 30 min, and chemiluminescent signal exposure for 5, 15, 30, 60, 120, 240, and 480 sec. Data analyses were performed using the Compass Software (ProteinSimple). Representative "virtual blot" electrophoretic images were automatically generated by the Compass Software (ProteinSimple). Each experiment was performed in technical triplicates with four to six biological replicates per phenotype.

2.4.2 Co-immunoprecipitation—Extracted synaptosomal protein from mPFC of HI and LI animals [Cohorts 3–5 (Fig. 6); Table 1] was subjected to immunoprecipitation (IP) techniques utilizing the Pierce™ Crosslink Magnetic IP/Co-IP kit (Thermo Fisher Scientific, Waltham, MA; catalog # 88805). The Pierce™ Crosslink Magnetic IP/Co-IP kit enables highly efficient IP by covalently crosslinking antibody to A/G magnetic beads. Briefly, 10 ug of PSD95 (Millipore, catalog # MAB1598) and SAP102 (Rockland Immunochemicals, Pottstown, PA; catalog # 200–301-G38) were bound and crosslinked to A/G magnetic beads using kit-provided coupling buffer and disuccinimidyl suberate (DSS). An elution buffer was used to remove non-crosslinked antibody and to quench the crosslinking reaction. The crosslinked beads were collected on a magnetic stand (DynaMag™; Thermo Fisher Scientific, catalog # 12321D) followed by addition of 500 ul of lysate solution (175 ug of mPFC synaptosomal protein + kit provided IP/Lysis buffer), rotated overnight at 4°C. The target antigen was heat eluted (95°C for 5 min) from the beads and immediately underwent traditional immunoblotting techniques. In brief, 30 ug of lP lysates and non-immunoprecipitated input lysates were loaded in precast gels (NuPage™ 4–12% Bis-Tris; Invitrogen, Carlsbad, CA; catalog # NP0335BOX), transferred to PVDF membranes, (Immun-Blot ® PVDF membranes; Bio-Rad, Hercules, CA; catalog # 162–0239) and blotted with GluN2A (1:1000; Abcam, Cambridge, UK; catalog # ab169873) or GluN2B (1:1000; Abcam, catalog # ab65783) overnight at 4°C. Membranes were incubated with mouse IgG IRDye 800 CW (1:10000) or rabbit IgG IRDye 680 RD (1:10000) for detection by Odyssey Imaging System (LI-COR, Lincoln, NE). The integrated intensity of each band was analyzed with the Odyssey Software and GluN2A and GluN2B immunoreactivity normalized to total immunoprecipitated PSD95 (1:1000) or SAP102 (1:100) immunoreactivity.

2.5 Statistical Analyses

Student's t-test was employed to analyze outcome measures of 1-CSRT task performance between phenotypes (HI versus LI) within each cohort, and an ordinary one-way analysis of variance (ANOVA) was employed to analyze each outcome measure from the 1-CSRT task performance across cohorts (Graphpad Prism 7). To evaluate the relationship between inherent motor impulsivity and 1-CSRT task performance following vehicle or DCS, a one-

way analysis of covariance (ANCOVA; quantitative covariate: target premature responses) was employed; treatment means were not adjusted for the influence of the covariate (i.e., adjusted p-values are not reported) (IBM SPSS Statistics). Student's t-test was employed to compare NMDAR subunit protein expression in HI versus LI rats, and Pearson's correlation was used to assess the relationship between premature responses, reinforcers earned, accuracy, or percent omissions and NMDAR subunit protein expression (Graphpad Prism 7).

3. Results

3.1 Identification of motor impulsivity phenotypes using the 1-CSRT Task

Table 1 illustrates the premature responses, reinforcers earned, accuracy, percent omissions, latency to respond, and time to finish the session on the ITI8 challenge observed across all five cohorts of HI and LI rats utilized in this study; each cohort is independently stratified to identify the phenotype. There was a main effect observed between cohorts on premature responses within LI rats ($F_{4,57}$=6. 15, p<0.05) and HI rats ($F_{4,58}$=25.40, p<0.05). Reinforcers earned ($F_{4,57}$=1.57, n.s.), percent omissions ($F_{4,57}$=0.47, n.s.), and time to finish ($F_{4,57}$=1.07, n.s.) did not differ within LI rats across Cohorts 1–5. A main effect on reinforcers earned ($F_{4,58}$=15.78, p<0.05), percent omissions ($F_{4,58}$=6.29, p<0.05), and time to finish ($F_{4,58}$=5.69, p<0.05) within HI rats alone was observed across Cohorts 1–5. Latency to respond did not differ between LI ($F_{4,57}$=1.66, n.s.) or HI ($F_{4,58}$=2.28, n.s.) rats across Cohorts 1–5. Accuracy averaged 95–98% between all cohorts (LI rats: F4,57 = 0.89, n.s.; HI rats: $F_{4,58}$=0.83, n.s.) and did not differ between phenotypes (Cohort 2: t_{23}=0.09, n.s.; Cohort 3: t_{28}=0.22, n.s.; Cohort 4: t_{28}=1.51, n.s.; Cohort 5: t_{21}=0.00, n.s.), except Cohort 1 (t_{15}=2.41, p<0.05). The difference in accuracy in Cohort 1 between HI and LI rats was marginal (approximately 2%) and did not affect task criteria or trainability (see Methods). As outbred rats are employed to identify the motor impulsivity phenotype, each cohort contains a unique group of animals in which naturally occurring variability is detectable between populations of animals [1, 49, 53, 54, 59]. Regardless, the defining characteristics between phenotypes were consistent and reproducible and individual rats between cohorts were not pooled for subsequent behavioral and/or biochemical analyses.

Levels of premature responses (Cohort 1: t_{15}=10.42, p<0.05; Cohort 2: t_{23}=12.14, p<0.05; Cohort 3: t_{28}=15.03, p<0.05; Cohort 4: t_{28}=9.14, p<0.05; Cohort 5: t_{21}=14.92, p<0.05), reinforcers earned (Cohort 1: t_{15}=7.39, p<0.05; Cohort 2: t_{23}=7.72, p<0.05; Cohort 3: t_{28}=6.55, p<0.05; Cohort 4: t_{28}=3.83, p<0.05; Cohort 5: t_{21}=3.61, p<0.05), percent omissions (Cohort 1: t_{15}=5.78, p<0.05; Cohort 2: t_{23}=4.25, p<0.05; Cohort 3: t_{28}=4.15, p<0.05; Cohort 4: t_{28}=5.18, p<0.05; Cohort 5: t_{21}=3.19, p<0.05), and time to finish (Cohort 1: t_{15}=5.99, p<0.05; Cohort 2: t_{23}=4.25, p<0.05; Cohort 3: t_{28}=4.69, p<0.05; Cohort 4: t_{28}=6.61, p<0.05; Cohort 5: t_{21}=2.85, p<0.05) were consistently different in HI versus LI rats (Table 1), as previously reported [48–53]. HI rats earned on average approximately 10 fewer reinforcers and displayed lower percent omissions relative to LI rats (Table 1), suggesting phenotypic differences in sensory, motor, and/or motivational factors play a role in the pattern of responding on the 1-CSRT task [48–55]. Due to the nature of the task parameters and pattern of responding, HI rats finished ITI8 sessions faster than LI rats across Cohorts 1–5. Taken together, the results across five independent cohorts of outbred rat

populations reflect the utility, reliability, and consistency of the 1-CSRT task to identify phenotypic differences in motor impulsivity.

3.2 Inherent motor impulsivity predicts responsiveness to systemic administration of D-cycloserine

We administered systemic DCS (1, 2, 5, 10, 20, and 50 mg/kg i.p.) following identification of inherent motor impulsivity. Target premature responses on the ITI8 challenge (i.e., inherent baseline motor impulsivity) predicted the number of premature responses (Fig. 1A; $F_{1,18}$= 5.52, p<0.05) but not the number of reinforcers earned (Fig. 1B; $F_{1,18}$=0.07, n.s.), accuracy (Fig. 1C; $F_{1,18}$=0.11, n.s.), or percent omissions (Fig. 1D; $F_{1,18}$=3.51, n.s.) following pretreatment with vehicle or DCS. Our simple interpretation is that baseline levels of premature responses are a significant factor in the observed DCS effectiveness on motor impulsivity and may indicate corresponding individual differences in NMDAR subunit composition and localization as a putative neurobiological substrate of inherent motor impulsivity.

3.3 Motor impulsivity predicts mPFC NMDAR subunit composition

To study the association of mPFC NMDAR subunit expression pattern upon inherent motor impulsivity, we probed for GluN1, GluN2A, and GluN2B in synaptosomal fractions from mPFC tissue of HI and LI animals (Figs. 2–4). HI rats exhibited lower mPFC synaptosomal GluN1 versus LI rats (Fig. 2A; t_9=2.39, p<0.05), and there was a negative correlation between premature responses and GluN1 protein expression (Fig. 2B; R=−0.540; p<0.05). There was no correlation between reinforcers earned (Fig. 2C; R=0.490; n.s.) or accuracy (Fig. 2D; R=−0.062; n.s.) but a positive correlation between percent omissions (Fig. 2E; R=0.597; p<0.05) and GluN1 protein expression. HI rats exhibited lower mPFC synaptosomal GluN2A versus LI rats (Fig. 3A; t_8=3.09, p<0.05); there was a negative correlation between premature responses and Glun2A protein expression (Fig. 3B; R= −0.658; p<0.05). There was a positive correlation between reinforcers earned (Fig. 3C; R=0.683; p<0.05), no correlation between accuracy (Fig. 3D; R=−0.109; n.s.), and a positive correlation between percent omissions (Fig. 3E; R=0.613; p<0.05) and GluN2A protein expression. HI rats exhibited higher levels of mPFC synaptosomal GluN2B versus LI rats (Fig. 4A; t_8=2.29, p<0.05), and there was a positive correlation between premature responses and GluN2B protein expression (Fig. 4B; R=0.550; p<0.05). There was no correlation between reinforcers earned (Fig. 4C; R=−0.537; n.s.), a positive correlation between accuracy and (Fig. 4D; R=0.586; p<0.05) and no correlation between percent omissions (Fig. 4E; R=−0.468; n.s.) and GluN2B protein expression. Thus, the NMDAR subunits are dynamically expressed within the mPFC of HI versus LI rats.

3.4 Motor impulsivity predicts GluN2B phosphorylation in the mPFC

We measured the mPFC synaptosomal protein expression of phosphorylated GluN2B (pGluN2B; Ser1303, C terminus) to study potential differential trafficking mechanisms of the GluN2B subunit [30, 62–64] in HI and LI rats. HI rats exhibited higher pGluN2B protein expression versus LI (Fig. 5A; t_9=2.59, p<0.05), and there was a positive correlation between premature responses and pGluN2B protein expression (Fig. 5B; R=0.700; p<0.05). There was a negative correlation between reinforcers earned (Fig. 5C; R=−.701; p<0.05) and

no correlation between accuracy (Fig. 5D; R=−0.514; n.s.) or percent omissions (Fig. 5E; R=−0.495; n.s.) and pGluN2B protein expression. These data suggest that GluN2B is phosphorylated to a greater degree at Ser1303 in highly impulsive rats.

3.5 Motor impulsivity is associated with mPFC NMDAR subunit synaptosomal stabilization and trafficking

We determined the association between PDZ proteins (i.e. PSD95 and SAP102) and GluN2 subunits in synaptosomal fraction from mPFC tissue of HI and LI animals. IP for PSD95 followed by immunoblot (IB) for GluN2A demonstrated approximately equal association between PSD95 and GluN2A in HI versus LI rats (Fig. 6A; t_{12}=0.99, n.s.). IP for PSD95 followed by IB for GluN2B revealed a greater association between PSD95 and GluN2B in HI versus LI rats (Fig. 6B; t_{13}=1.91, p<0.05). IP for SAP102 and IB for GluN2B yielded a greater association between SAP102 and GluN2B in HI versus LI rats (Fig. 6C; t_{12}=1.78, p<0.05). Taken together, HI rats exhibit higher levels of GluN2B:MAGUK interactions suggesting differences between the trafficking and targeting of the GluN2B subunit may distinguish phenotypic levels of motor impulsivity.

4. Discussion

In summary, identification of the motor impulsivity phenotype is stable and consistent in the 1-CSRT task. Inherent motor impulsivity predicted responsiveness to DCS which prompted further studies to determine NMDAR subunit expression in synaptosomal compartments of the mPFC. We observed lower GluN1 and GluN2A subunit protein expression, but higher GluN2B subunit protein expression in HI versus LI rats. Premature responses were negatively correlated with both GluN1 and GluN2A synaptosomal protein expression within the mPFC while omissions were positively correlated. These measures provide an indication that sensory and/or motivational factors, i.e., goal-directed behaviors, are associated with the status of the NMDAR complex and provide additional insight into the multifaceted determinants of the trait of motor impulsivity [48–53]. We also discovered higher pGluN2B in the mPFC of HI versus LI rats, which may indicate potential trafficking mechanisms underlie differences in NMDAR subunit expression in HI versus LI rats. Additionally, we detected differential protein:protein associations between synaptic scaffolding proteins PSD95 and SAP102 and GluN2 subunits in the mPFC of HI versus LI rats. Specifically, there was a higher association between PSD95 and GluN2B and SAP102 and GluN2B in HI versus LI animals; interestingly, there was approximately equal association between PSD95 and GluN2A in HI versus LI animals. Taken together, these data indicate that there is a possible transformation of the mPFC NMDAR subunit expression pattern and/or synaptosomal localization that may underlie high inherent motor impulsivity.

Pharmacological manipulation of NMDAR demonstrated that inherent levels of motor impulsivity predicted dynamic responses to DCS-induced impulsivity. Further, we noted a modest overall decrease in impulsivity at the lowest dose of DCS and increased impulsivity at the highest dose of DCS tested. These data are likely a reflection of the partial agonist activity of DCS, where at lower doses, it performs as an agonist, and at higher doses, it performs as an antagonist [46, 47], and align with studies which demonstrated increased

impulsivity following NMDAR antagonism [33, 36–42] and intra-mPFC NMDAR antagonism [39, 40]. While the precise mechanisms involved are not clearly understood, in the present study, we demonstrated differences in cortical NMDAR subunit expression and identified possible NMDAR-trafficking and -localization mechanisms that may elucidate the complex neurobiology of impulsivity and responsiveness to NMDAR ligands. Taken together, the fundamental role for the mPFC in motor impulsivity, which is coordinated by the regulatory capacity of multiple neurotransmitters and effectors (e.g., dopamine and serotonin system [1, 2, 48, 49, 65–68]), includes the NMDAR system and suggests that the NMDAR subunit protein profile may be important in laying the foundation for individual differences in motor impulsivity.

Interestingly, GluN2B synaptosomal protein expression was higher in the mPFC of HI rats, and premature responses were positively correlated with GluN2B protein expression. The GluN2B subunit is highly expressed in immature neurons and at nascent synapses at birth and into early childhood but decreases in expression during adulthood; congruently the GluN2A subunit protein expression increases with age as neurons mature [25, 69–71]. Further, GluN2A-containing NMDARs mediate long-term potentiation (LTP), while GluN2B-containing NMDARs are purported to play a greater role in long-term depression or weakening of synaptic strength [72], but this is not always the case. For example, switching synaptic GluN2B-containing NMDARs that bind to CAMKII (Ca^{2+}/calmodulin kinase II) with GluN2A-containing NMDARs that bind to CAMKII results in a significant decrease of LTP [73] suggesting that GluN2B, through its interactions with CAMKII, may induce LTP. Therefore, it is possible that the observed higher mPFC GluN2B discovered herein is a homeostatic feedback mechanism in response to lower levels of GluN1 and GluN2A in HI rats. It is also plausible that the “switch” from GluN2B to GluN2A-containing NMDARs during development was impaired, resulting in higher levels of GluN2B into adulthood. These are areas of active research in our laboratory and the focus of future studies.

The GluN2B subunit may play a more defined role in regulating synaptic plasticity [74, 75] and is more synaptically fluid than the GluN2A subunit [76–78], possibly due to phosphorylation [30]. Excitingly, we discovered phosphorylation of the GluN2B Ser1303 was higher in HI versus LI rats and that premature responses positively correlated with pGluN2B protein expression. There are several known serine/threonine phosphorylation sites on NMDAR subunits [30] which are regulated by various protein kinases [79, 80]. Further, each kinase may exert a unique effect; for example, phosphorylation via protein kinase C (PKC) can increase NMDAR channel opening rates and upregulate NMDAR surface expression [81, 82]. Additionally, PKC activation can mediate NMDAR synaptic targeting [83]. CAMKII is also heavily involved in regulating NMDAR localization and binds to GluN2B with greater affinity than GluN2A [62, 73, 84–87]. GluN2B-CAMKII complexes are targeted to the synapse and maintain synaptic strength [88]. Ser1303, a phosphorylation site on the C-terminus of GluN2B that interacts with both PKC and CAMKII, is involved in both potentiating and deactivating GluN2B currents [62, 63, 89]. Further, phosphorylation can inhibit or potentiate NMDAR-PDZ protein complexes to therefore regulate synaptic localization and trafficking of the NMDAR subunits within the synapse [28, 88, 90]. Taken together, these data suggest that phosphorylation at the GluN2B

Ser1303 site may be involved in elevated synaptic trafficking of GluN2B in the mPFC of HI rats, and support future studies investigating the complex mechanisms mediating phosphorylation events of the NMDAR subunits.

PDZ proteins associated with GluN2 subunits are involved in synaptic stabilization and receptor mobility [26–29]. Both PSD95 and SAP102 will drive GluN2B to the synapse, but SAP102, in particular, is associated with enhanced receptor mobility [27–29]. Further, SAP102 is preferentially associated with GluN2B [26, 28] and its association enhances mobility and surface delivery of GluN2B over GluN2A [24]. In fact, there is a secondary non-PDZ interaction site specific to GluN2B and SAP102 that is involved in synaptic mobilization of GluN2B [28]. As HI rats had higher GluN2B:PSD95 and GluN2B:SAP102 protein:protein interactions, we propose there is an enhanced stabilization and trafficking of GluN2B in HI versus LI rats. Interestingly, there was equal association of GluN2A:PSD95 between phenotypes, thus, it is possible that the GluN2A differences observed in HI versus LI rats may be caused by partnering (or lack thereof) of GluN2A to an alternative synaptic scaffolding protein (e.g. PSD93).

Overall, our present work demonstrates a distinct neurobiology of the NMDAR, i.e. subunit expression and trafficking, in the cortical synaptosomal environment to govern the motor impulsivity phenotype. Increased understanding of the complex regulation of NMDAR balance within the mPFC as it relates to motor impulsivity may lead to a better understanding of risk factors and treatments for several neuropsychiatric disorders.

Acknowledgements

We thank Christopher A. Krebs, Ph.D. for his technical contributions to the behavioral and biochemical experiments of the initial cohort of rats, as well as Mr. Dennis J. Sholler for his insightful comments on the manuscript.

5. Conflict of Interest/Financial Support

This work was supported by NIDA grants R00 DA033374 (N.C.A.) and T32 DA007287 (B.D.D.R.). All authors declare no conflicts of interest.

7. Literature Cited

[1]. Anastasio NC, Stutz SJ, Fink LH, Swinford-Jackson SE, Sears RM, DiLeone RJ, Rice KC, Moeller FG, Cunningham KA, Serotonin (5-HT) 5-HT2A Receptor (5-HT2AR):5-HT2CR Imbalance in Medial Prefrontal Cortex Associates with Motor Impulsivity, ACS Chem Neurosci 6(7) (2015) 1248–58. [PubMed: 26120876]

[2]. Winstanley CA, The utility of rat models of impulsivity in developing pharmacotherapies for impulse control disorders, Br.J.Pharmacol 164 (2011) 1301–1321. [PubMed: 21410459]

[3]. Dalley JW, Roiser JP, Dopamine, serotonin and impulsivity, Neuroscience 215 (2012) 42–58. [PubMed: 22542672]

[4]. Patton JH, Stanford MS, Barratt ES, Factor structure of the Barratt impulsiveness scale, J.Clin.Psychol 51(6) (1995) 768–774. [PubMed: 8778124]

[5]. Moeller FG, Dougherty DM, Barratt ES, Schmitz JM, Swann AC, Grabowski J, The impact of impulsivity on cocaine use and retention in treatment, J.Subst.Abuse Treat 21(4) (2001) 193–198. [PubMed: 11777668]

[6]. Weafer J, Baggott MJ, de Wit H, Test-retest reliability of behavioral measures of impulsive choice, impulsive action, and inattention, Experimental and clinical psychopharmacology 21(6) (2013) 475–81. [PubMed: 24099351]

[7]. Hamilton KR, Littlefield AK, Anastasio NC, Cunningham KA, Fink LH, Wing VC, Mathias CW, Lane SD, Schutz CG, Swann AC, Lejuez CW, Clark L, Moeller FG, Potenza MN, Rapid-response impulsivity: definitions, measurement issues, and clinical implications, Personal Disord 6(2) (2015) 168–81. [PubMed: 25867840]

[8]. Voon V, Models of Impulsivity with a Focus on Waiting Impulsivity: Translational Potential for Neuropsychiatric Disorders, Curr Addict Rep 1(4) (2014) 281–288. [PubMed: 25346881]

[9]. Hamilton KR, Mitchell MR, Wing VC, Balodis IM, Bickel WK, Fillmore M, Lane SD, Lejuez CW, Littlefield AK, Luijten M, Mathias CW, Mitchell SH, Napier TC, Reynolds B, Schutz CG, Setlow B, Sher KJ, Swann AC, Tedford SE, White MJ, Winstanley CA, Yi R, Potenza MN, Moeller FG, Choice impulsivity: Definitions, measurement issues, and clinical implications, Personal Disord 6(2) (2015) 182–98. [PubMed: 25867841]

[10]. Euston DR, Gruber AJ, McNaughton BL, The role of medial prefrontal cortex in memory and decision making, Neuron 76(6) (2012) 1057–70. [PubMed: 23259943]

[11]. Grabenhorst F, Rolls ET, Value, pleasure and choice in the ventral prefrontal cortex, Trends Cogn Sci 15(2) (2011) 56–67. [PubMed: 21216655]

[12]. Jackson ME, Homayoun H, Moghaddam B, NMDA receptor hypofunction produces concomitant firing rate potentiation and burst activity reduction in the prefrontal cortex, Proc Natl Acad Sci U S A 101(22) (2004) 8467–72. [PubMed: 15159546]

[13]. Monyer H, Sprengel R, Schoepfer R, Herb A, Higuchi M, Lomeli H, Burnashev N, Sakmann B, Seeburg PH, Heteromeric NMDA receptors: molecular and functional distinction of subtypes, Science 256(5060) (1992) 1217–21. [PubMed: 1350383]

[14]. Cull-Candy SG, Leszkiewicz DN, Role of distinct NMDA receptor subtypes at central synapses, Sci STKE 2004(255) (2004) re16. [PubMed: 15494561]

[15]. Del AA, Mora F, Prefrontal cortex-nucleus accumbens interaction: in vivo modulation by dopamine and glutamate in the prefrontal cortex, Pharmacol.Biochem.Behav 90(2) (2008) 226–235. [PubMed: 18508116]

[16]. Johnson JW, Ascher P, Glycine potentiates the NMDA response in cultured mouse brain neurons, Nature 325(6104) (1987) 529–31. [PubMed: 2433595]

[17]. Lau CG, Zukin RS, NMDA receptor trafficking in synaptic plasticity and neuropsychiatric disorders, Nat Rev Neurosci 8(6) (2007) 413–26. [PubMed: 17514195]

[18]. Ivanov A, Pellegrino C, Rama S, Dumalska I, Salyha Y, Ben-Ari Y, Medina I, Opposing role of synaptic and extrasynaptic NMDA receptors in regulation of the extracellular signal-regulated kinases (ERK) activity in cultured rat hippocampal neurons, J Physiol 572(Pt 3) (2006) 789–98. [PubMed: 16513670]

[19]. Kim E, Sheng M, PDZ domain proteins of synapses, Nat Rev Neurosci 5(10) (2004) 771–81. [PubMed: 15378037]

[20]. Prybylowski K, Chang K, Sans N, Kan L, Vicini S, Wenthold RJ, The synaptic localization of NR2B-containing NMDA receptors is controlled by interactions with PDZ proteins and AP-2, Neuron 47(6) (2005) 845–57. [PubMed: 16157279]

[21]. Mauceri D, Gardoni F, Marcello E, Di LM, Dual role of CaMKII-dependent SAP97 phosphorylation in mediating trafficking and insertion of NMDA receptor subunit NR2A, J.Neurochem. 100(4) (2007) 1032–1046. [PubMed: 17156128]

[22]. Wu LJ, Xu H, Ren M, Cao X, Zhuo M, Pharmacological isolation of postsynaptic currents mediated by NR2A- and NR2B-containing NMDA receptors in the anterior cingulate cortex, Mol Pain 3 (2007) 11. [PubMed: 17470281]

[23]. Wenthold RJ, Prybylowski K, Standley S, Sans N, Petralia RS, Trafficking of NMDA receptors, Annu Rev Pharmacol Toxicol 43 (2003) 335–58. [PubMed: 12540744]

[24]. Sans N, Prybylowski K, Petralia RS, Chang K, Wang YX, Racca C, Vicini S, Wenthold RJ, NMDA receptor trafficking through an interaction between PDZ proteins and the exocyst complex, Nature cell biology 5(6) (2003) 520–30. [PubMed: 12738960]

[25]. Monyer H, Burnashev N, Laurie DJ, Sakmann B, Seeburg PH, Developmental and regional expression in the rat brain and functional properties of four NMDA receptors, Neuron 12(3) (1994) 529–40. [PubMed: 7512349]

[26]. Sans N, Petralia RS, Wang YX, Blahos J, 2nd, J.W. Hell, R.J. Wenthold, A developmental change in NMDA receptor-associated proteins at hippocampal synapses, J Neurosci 20(3) (2000) 1260–71. [PubMed: 10648730]

[27]. Zheng CY, Petralia RS, Wang YX, Kachar B, Wenthold RJ, SAP102 is a highly mobile MAGUK in spines, J Neurosci 30(13) (2010) 4757–66. [PubMed: 20357126]

[28]. Chen BS, Gray JA, Sanz-Clemente A, Wei Z, Thomas EV, Nicoll RA, Roche KW, SAP102 mediates synaptic clearance of NMDA receptors, Cell Rep 2(5) (2012) 1120–8. [PubMed: 23103165]

[29]. Groc L, Heine M, Cousins SL, Stephenson FA, Lounis B, Cognet L, Choquet D, NMDA receptor surface mobility depends on NR2A-2B subunits, Proc Natl Acad Sci U S A 103(49) (2006) 18769–74. [PubMed: 17124177]

[30]. Chen BS, Roche KW, Regulation of NMDA receptors by phosphorylation, Neuropharmacology 53(3) (2007) 362–8. [PubMed: 17644144]

[31]. Lee HK, Synaptic plasticity and phosphorylation, Pharmacol Ther 112(3) (2006) 810–32. [PubMed: 16904750]

[32]. Egerton A, Reid L, McKerchar CE, Morris BJ, Pratt JA, Impairment in perceptual attentional set-shifting following PCP administration: a rodent model of set-shifting deficits in schizophrenia, Psychopharmacology (Berl) 179(1) (2005) 77–84. [PubMed: 15682304]

[33]. Higgins GA, Ballard TM, Huwyler J, Kemp JA, Gill R, Evaluation of the NR2B-selective NMDA receptor antagonist Ro 63–1908 on rodent behaviour: evidence for an involvement of NR2B NMDA receptors in response inhibition, Neuropharmacology 44(3) (2003) 324–341. [PubMed: 12604092]

[34]. Jentsch JD, Roth RH, The neuropsychopharmacology of phencyclidine: from NMDA receptor hypofunction to the dopamine hypothesis of schizophrenia, Neuropsychopharmacology 20(3) (1999) 201–25. [PubMed: 10063482]

[35]. Le Pen G, Grottick AJ, Higgins GA, Moreau JL, Phencyclidine exacerbates attentional deficits in a neurodevelopmental rat model of schizophrenia, Neuropsychopharmacology 28(10) (2003) 1799–809. [PubMed: 12784101]

[36]. Mirjana C, Baviera M, Invernizzi RW, Balducci C, The serotonin 5-HT2A receptors antagonist M100907 prevents impairment in attentional performance by NMDA receptor blockade in the rat prefrontal cortex, Neuropsychopharmacology 29(9) (2004) 1637–1647. [PubMed: 15127084]

[37]. Nikiforuk A, Holuj M, Potasiewicz A, Popik P, Effects of the selective 5-HT7 receptor antagonist SB-269970 on premature responding in the five-choice serial reaction time test in rats, Behav Brain Res 289 (2015) 149–56. [PubMed: 25930219]

[38]. Burton CL, Fletcher PJ, Age and sex differences in impulsive action in rats: the role of dopamine and glutamate, Behav Brain Res 230(1) (2012) 21–33. [PubMed: 22326372]

[39]. Agnoli L, Carli M, Dorsal-striatal 5-HT(2)A and 5-HT(2)C receptors control impulsivity and perseverative responding in the 5-choice serial reaction time task, Psychopharmacology (Berl) 219(2) (2012) 633–45. [PubMed: 22113450]

[40]. Murphy ER, Fernando AB, Urcelay GP, Robinson ES, Mar AC, Theobald DE, Dalley JW, Robbins TW, Impulsive behaviour induced by both NMDA receptor antagonism and GABAA receptor activation in rat ventromedial prefrontal cortex, Psychopharmacology (Berl) 219(2) (2012) 401–10. [PubMed: 22101355]

[41]. Smith JW, Gastambide F, Gilmour G, Dix S, Foss J, Lloyd K, Malik N, Tricklebank M, A comparison of the effects of ketamine and phencyclidine with other antagonists of the NMDA receptor in rodent assays of attention and working memory, Psychopharmacology (Berl) 217(2) (2011) 255–69. [PubMed: 21484239]

[42]. Benn A, Robinson ES, Investigating glutamatergic mechanism in attention and impulse control using rats in a modified 5-choice serial reaction time task, PLoS One 9(12) (2014) e115374. [PubMed: 25526617]

[43]. Pozzi L, Baviera M, Sacchetti G, Calcagno E, Balducci C, Invernizzi RW, Carli M, Attention deficit induced by blockade of N-methyl D-aspartate receptors in the prefrontal cortex is associated with enhanced glutamate release and cAMP response element binding protein

phosphorylation: role of metabotropic glutamate receptors 2/3, Neuroscience 176 (2011) 336–48. [PubMed: 21193020]

[44]. Cottone P, Iemolo A, Narayan AR, Kwak J, Momaney D, Sabino V, The uncompetitive NMDA receptor antagonists ketamine and memantine preferentially increase the choice for a small, immediate reward in low-impulsive rats, Psychopharmacology (Berl) 226(1) (2013) 127–38. [PubMed: 23104264]

[45]. Schade S, Paulus W, D-Cycloserine in Neuropyschiatric Diseases: A Systematic Review, International Journal of Neuropsychopharmacology 19(4) (2016) 1–7.

[46]. Gomes FV, Kakihata AM, Semedo AC, Hott SC, Uliana DL, Guimaraes FS, Resstel LB, D-cycloserine injected into the dorsolateral periaqueductal gray induces anxiolytic-like effects in rats, Behav Brain Res 271 (2014) 374–9. [PubMed: 24931794]

[47]. Lanthorn TH, D-Cycloserine: Agonist turned antagonist, Amino Acids 6(3) (1994) 247–60. [PubMed: 24189733]

[48]. Anastasio NC, Stutz SJ, Fox RG, Sears RM, Emeson RB, DiLeone RJ, O'Neil RT, Fink LH, Li D, Green TA, Moeller FG, Cunningham KA, Functional status of the serotonin 5-HT2C receptor (5-HT2CR) drives interlocked phenotypes that precipitate relapse-like behaviors in cocaine dependence, Neuropsychopharmacology 39(2) (2014) 370–82. [PubMed: 23939424]

[49]. Fink LH, Anastasio NC, Fox RG, Rice KC, Moeller FG, Cunningham KA, Individual Differences in Impulsive Action Reflect Variation in the Cortical Serotonin 5-HT2A Receptor System, Neuropsychopharmacology 40(8) (2015) 1957–68. [PubMed: 25666313]

[50]. Anastasio NC, Stoffel EC, Fox RG, Bubar MJ, Rice KC, Moeller FG, Cunningham KA, Serotonin (5-hydroxytryptamine) 5-HT_{2A} receptor: Association with inherent and cocaine-evoked behavioral disinhibition in rats, Behav.Pharmacol. 22(3) (2011) 248–261. [PubMed: 21499079]

[51]. Cunningham KA, Anastasio NC, Fox RG, Stutz SJ, Bubar MJ, Swinford SE, Watson CS, Gilbertson SR, Rice KC, Rosenzweig-Lipson S, Moeller FG, Synergism between a serotonin 5-HT2A receptor (5-HT2AR) antagonist and 5-HT2CR agonist suggests new pharmacotherapeutics for cocaine addiction, ACS Chemical Neuroscience 4 (2013) 110–121. [PubMed: 23336050]

[52]. Anastasio NC, Gilbertson SR, Bubar MJ, Agarkov A, Stutz SJ, Jeng Y, Bremer NM, Smith TD, Fox RG, Swinford SE, Seitz PK, Charendoff MN, Craft JW Jr., Laezza FM, Watson CS, Briggs JM, Cunningham KA, Peptide inhibitors disrupt the serotonin 5-HT2C receptor interaction with phosphatase and tensin homolog to allosterically modulate cellular signaling and behavior, J Neurosci 33(4) (2013) 1615–30. [PubMed: 23345234]

[53]. Sholler DJ, Stutz SJ, Fox RG, Boone EL, Wang Q, Rice KC, Moeller FG, Anastasio NC, Cunningham KA, The 5-HT2A Receptor (5-HT2AR) Regulates Impulsive Action and Cocaine Cue Reactivity in Male Sprague-Dawley Rats, J Pharmacol Exp Ther 368(1) (2019) 41–49. [PubMed: 30373886]

[54]. Anastasio NC, Stutz SJ, Price AE, Davis-Reyes BD, Sholler DJ, Ferguson SM, Neumaier JF, Moeller FG, Hommel JD, Cunningham KA, Convergent neural connectivity in motor impulsivity and high-fat food binge-like eating in male Sprague-Dawley rats, Neuropsychopharmacology (2019).

[55]. Robbins TW, The 5-choice serial reaction time task: behavioural pharmacology and functional neurochemistry, Psychopharmacology (Berl) 163(3–4) (2002) 362–380. [PubMed: 12373437]

[56]. Dalley JW, Theobald DE, Eagle DM, Passetti F, Robbins TW, Deficits in impulse control associated with tonically-elevated serotonergic function in rat prefrontal cortex, Neuropsychopharmacology 26(6) (2002) 716–728. [PubMed: 12007742]

[57]. Heffner TG, Hartman JA, Seiden LS, Rapid method for the regional dissection of the rat brain, Pharmacol.Biochem.Behav. 13 (1980) 453–456. [PubMed: 7422701]

[58]. Anastasio NC, Lanfranco MF, Bubar MJ, Seitz PK, Stutz SJ, McGinnis AG, Watson CS, Cunningham KA, Serotonin 5-HT2C receptor protein expression is enriched in synaptosomal and post-synaptic compartments of rat cortex, J Neurochem 113(6) (2010) 1504–15. [PubMed: 20345755]

[59]. Anastasio NC, Liu S, Maili L, Swinford SE, Lane SD, Fox RG, Hamon SC, Nielsen DA, Cunningham KA, Moeller FG, Variation within the serotonin (5-HT) 5-HT(2)C receptor system

aligns with vulnerability to cocaine cue reactivity, Translational psychiatry 4 (2014) e369. [PubMed: 24618688]

[60]. Swinford-Jackson SE, Anastasio NC, Fox RG, Stutz SJ, Cunningham KA, Incubation of cocaine cue reactivity associates with neuroadaptations in the cortical serotonin (5-HT) 5-HT2C receptor (5-HT2CR) system, Neuroscience 324 (2016) 50–61. [PubMed: 26926963]

[61]. Paxinos G, Watson C, The Rat Brain in Stereotaxic Coordinates, 4 ed., Academic Press, Sydney, 1998.

[62]. Strack S, Robison AJ, Bass MA, Colbran RJ, Association of calcium/calmodulin-dependent kinase II with developmentally regulated splice variants of the postsynaptic density protein densin-180, J Biol Chem 275(33) (2000) 25061–4. [PubMed: 10827168]

[63]. Liao GY, Wagner DA, Hsu MH, Leonard JP, Evidence for direct protein kinase-C mediated modulation of N-methyl-D-aspartate receptor current, Mol Pharmacol 59(5) (2001) 960–4. [PubMed: 11306676]

[64]. Liu XY, Chu XP, Mao LM, Wang M, Lan HX, Li MH, Zhang GC, Parelkar NK, Fibuch EE, Haines M, Neve KA, Liu F, Xiong ZG, Wang JQ, Modulation of D2R-NR2B interactions in response to cocaine, Neuron 52(5) (2006) 897–909. [PubMed: 17145509]

[65]. Pattij T, Vanderschuren LJ, The neuropharmacology of impulsive behaviour, Trends Pharmacol.Sci. 29(4) (2008) 192–199. [PubMed: 18304658]

[66]. Cunningham KA, Anastasio NC, Serotonin at the nexus of impulsivity and cue reactivity in cocaine addiction, Neuropharmacology 76 Pt B (2014) 460–78. [PubMed: 23850573]

[67]. Besson M, Pelloux Y, Dilleen R, Theobald DE, Lyon A, Belin-Rauscent A, Robbins TW, Dalley JW, Everitt BJ, Belin D, Cocaine modulation of frontostriatal expression of Zif268, D2, and 5-HT2c receptors in high and low impulsive rats, Neuropsychopharmacology 38(10) (2013) 1963–73. [PubMed: 23632436]

[68]. Simon NW, Beas BS, Montgomery KS, Haberman RP, Bizon JL, Setlow B, Prefrontal cortical-striatal dopamine receptor mRNA expression predicts distinct forms of impulsivity, Eur J Neurosci 37(11) (2013) 1779–88. [PubMed: 23510331]

[69]. Dumas TC, Developmental regulation of cognitive abilities: modified composition of a molecular switch turns on associative learning, Prog Neurobiol 76(3) (2005) 189–211. [PubMed: 16181726]

[70]. Kirson ED, Yaari Y, Synaptic NMDA receptors in developing mouse hippocampal neurones: functional properties and sensitivity to ifenprodil, J Physiol 497 (Pt 2) (1996) 437–55. [PubMed: 8961186]

[71]. Yashiro K, Philpot BD, Regulation of NMDA receptor subunit expression and its implications for LTD, LTP, and metaplasticity, Neuropharmacology 55(7) (2008) 1081–94. [PubMed: 18755202]

[72]. Kim MJ, Dunah AW, Wang YT, Sheng M, Differential roles of NR2A- and NR2B-containing NMDA receptors in Ras-ERK signaling and AMPA receptor trafficking, Neuron 46(5) (2005) 745–60. [PubMed: 15924861]

[73]. Barria A, Malinow R, NMDA receptor subunit composition controls synaptic plasticity by regulating binding to CaMKII, Neuron 48(2) (2005) 289–301. [PubMed: 16242409]

[74]. Hanson JE, Pare JF, Deng L, Smith Y, Zhou Q, Altered GluN2B NMDA receptor function and synaptic plasticity during early pathology in the PS2APP mouse model of Alzheimer's disease, Neurobiol Dis 74 (2015) 254–62. [PubMed: 25484285]

[75]. Shipton OA, Paulsen O, GluN2A and GluN2B subunit-containing NMDA receptors in hippocampal plasticity, Philosophical transactions of the Royal Society of London. Series B, Biological sciences 369(1633) (2014) 20130163.

[76]. Lavezzari G, McCallum J, Dewey CM, Roche KW, Subunit-specific regulation of NMDA receptor endocytosis, J Neurosci 24(28) (2004) 6383–91. [PubMed: 15254094]

[77]. Roche KW, Standley S, McCallum J, Dune Ly C, Ehlers MD, Wenthold RJ, Molecular determinants of NMDA receptor internalization, Nat Neurosci 4(8) (2001) 794–802. [PubMed: 11477425]

[78]. Scott DB, Michailidis I, Mu Y, Logothetis D, Ehlers MD, Endocytosis and degradative sorting of NMDA receptors by conserved membrane-proximal signals, J Neurosci 24(32) (2004) 7096–109. [PubMed: 15306643]

[79]. Mammen AL, Kamboj S, Huganir RL, Protein phosphorylation of ligand-gated ion channels, Methods in enzymology 294 (1999) 353–70. [PubMed: 9916238]

[80]. Roche KW, Tingley WG, Huganir RL, Glutamate receptor phosphorylation and synaptic plasticity, Current opinion in neurobiology 4(3) (1994) 383–8. [PubMed: 7919933]

[81]. Lan JY, Skeberdis VA, Jover T, Grooms SY, Lin Y, Araneda RC, Zheng X, Bennett MV, Zukin RS, Protein kinase C modulates NMDA receptor trafficking and gating, Nat Neurosci 4(4) (2001) 382–90. [PubMed: 11276228]

[82]. Lu WY, Xiong ZG, Lei S, Orser BA, Dudek E, Browning MD, MacDonald JF, G-protein-coupled receptors act via protein kinase C and Src to regulate NMDA receptors, Nat Neurosci 2(4) (1999) 331–8. [PubMed: 10204539]

[83]. Crump FT, Dillman KS, Craig AM, cAMP-dependent protein kinase mediates activity-regulated synaptic targeting of NMDA receptors, J Neurosci 21(14) (2001) 5079–88. [PubMed: 11438583]

[84]. Bayer KU, De Koninck P, Leonard AS, Hell JW, Schulman H, Interaction with the NMDA receptor locks CaMKII in an active conformation, Nature 411(6839) (2001) 801–5. [PubMed: 11459059]

[85]. Leonard AS, Lim IA, Hemsworth DE, Horne MC, Hell JW, Calcium/calmodulin-dependent protein kinase II is associated with the N-methyl-D-aspartate receptor, Proc Natl Acad Sci U S A 96(6) (1999) 3239–44. [PubMed: 10077668]

[86]. Mayadevi M, Praseeda M, Kumar KS, Omkumar RV, Sequence determinants on the NR2A and NR2B subunits of NMDA receptor responsible for specificity of phosphorylation by CaMKII, Biochimica et biophysica acta 1598(1–2) (2002) 40–5. [PubMed: 12147342]

[87]. Strack S, Colbran RJ, Autophosphorylation-dependent targeting of calcium/ calmodulin-dependent protein kinase II by the NR2B subunit of the N-methyl- D-aspartate receptor, J Biol Chem 273(33) (1998) 20689–92. [PubMed: 9694809]

[88]. Barcomb K, Hell JW, Benke TA, Bayer KU, The CaMKII/GluN2B Protein Interaction Maintains Synaptic Strength, J Biol Chem 291(31) (2016) 16082–9. [PubMed: 27246855]

[89]. Tavalin SJ, Colbran RJ, CaMKII-mediated phosphorylation of GluN2B regulates recombinant NMDA receptor currents in a chloride-dependent manner, Molecular and cellular neurosciences 79 (2017) 45–52. [PubMed: 27998718]

[90]. Sanz-Clemente A, Matta JA, Isaac JT, Roche KW, Casein kinase 2 regulates the NR2 subunit composition of synaptic NMDA receptors, Neuron 67(6) (2010) 984–96. [PubMed: 20869595]

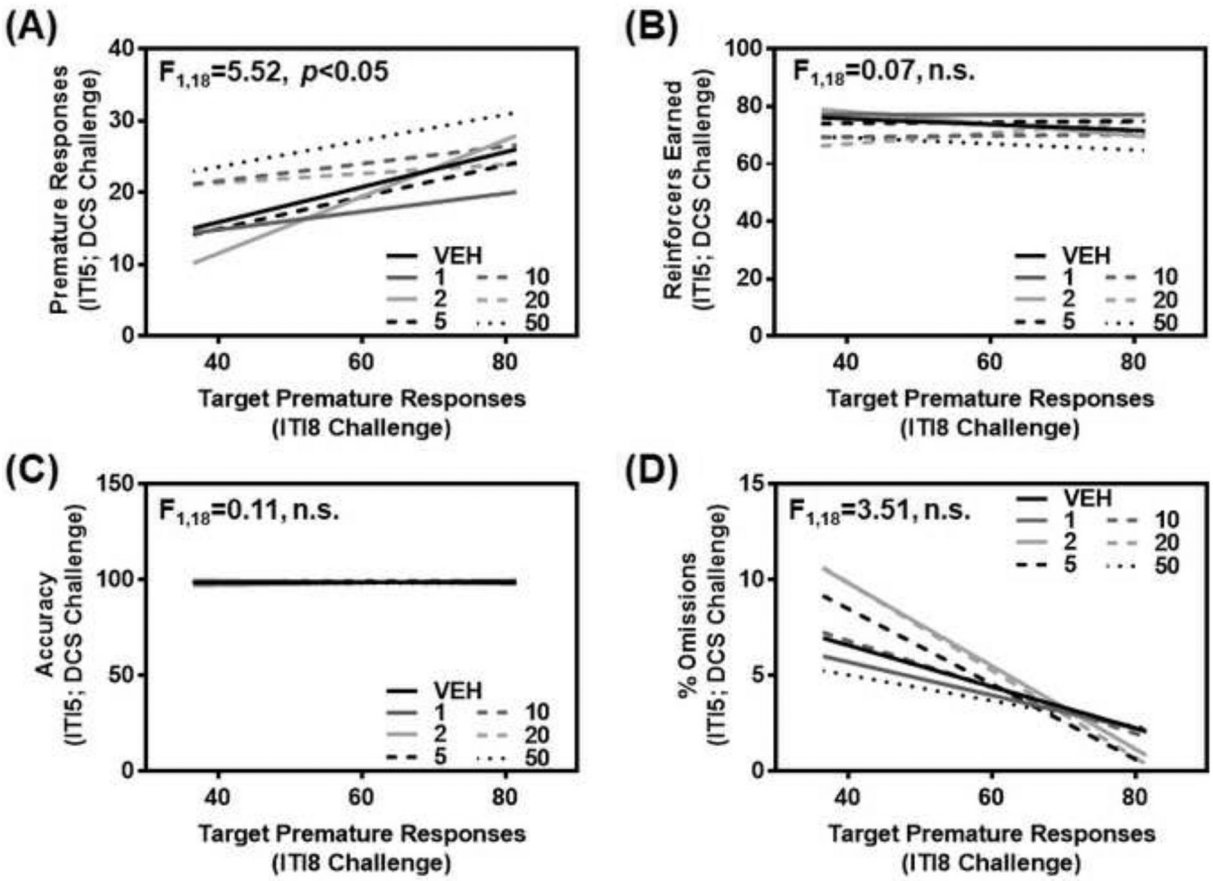

Figure 1. Inherent motor impulsivity predicts premature responses to D-cycloserine, but not additional measures from the 1-CSRT task.

(A) Target premature responses on the ITI8 challenge session (baseline impulsivity) predicted responsiveness to D-cycloserine (1, 2, 5, 10, 20, or 50 mg/kg i.p.; 15 min pretreatment) during the ITI5 maintenance sessions ($p<0.05$). Inherent motor impulsivity was not a predictive factor for **(B)** reinforcers earned (n.s.), **(C)** accuracy (n.s.), or **(D)** percent omissions (n.s.). The relationship between 1-CSRT task measures on an ITI8 challenge and ITI5 session for each pretreatment condition with vehicle or D-cycloserine is represented by a linear regression line.

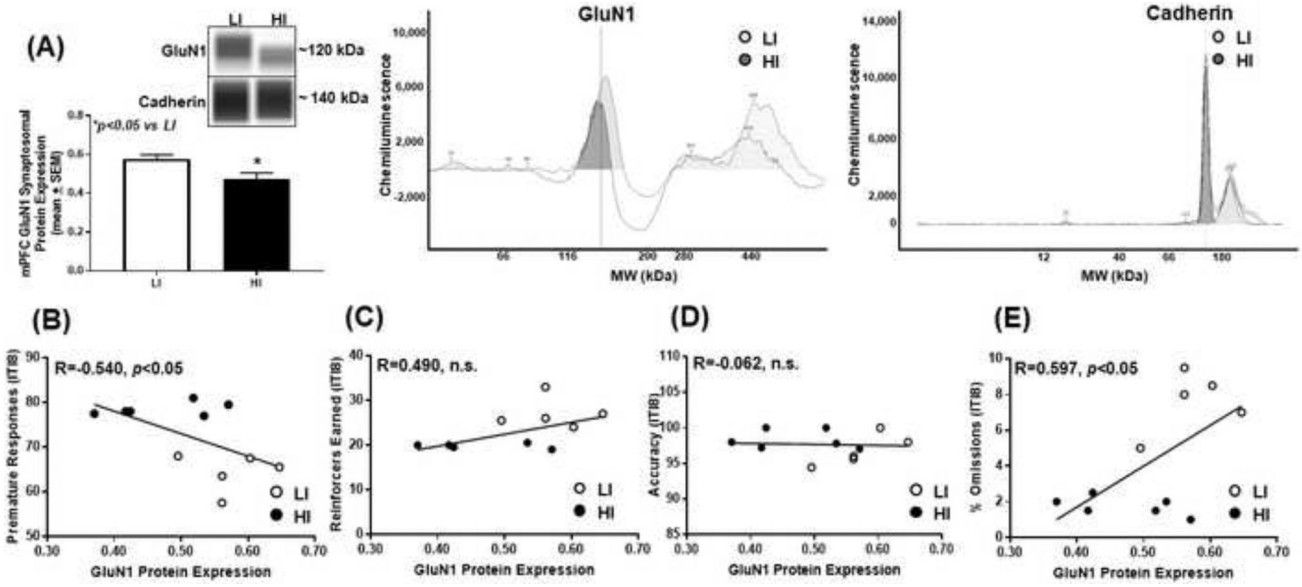

Figure 2. High trait motor impulsivity corresponds to lower GluN1 expression and correlates with additional measures from the 1-CSRT task.

(A) HI rats exhibit lower GluN1 versus LI rat (*p<0.05 *vs.* LI). Virtual blot-like representative images generated directly from the chemiluminescent signal for the GluN1 and cadherin loading control were performed using crude synaptosomal protein from the mPFC (**inset**). The corresponding electropherograms with chemiluminescent signals for GluN1 and cadherin represents HI (dark grey) and LI (light grey) rats. Correlational analyses between **(B)** premature responses (R=−0.540; p<0.05), **(C)** reinforcers earned (R=0.490; n.s.), **(D)** accuracy (R=−0.062; n.s.) and **(E)** percent omissions (R=0.597; p<0.05) and GluN1 protein expression.

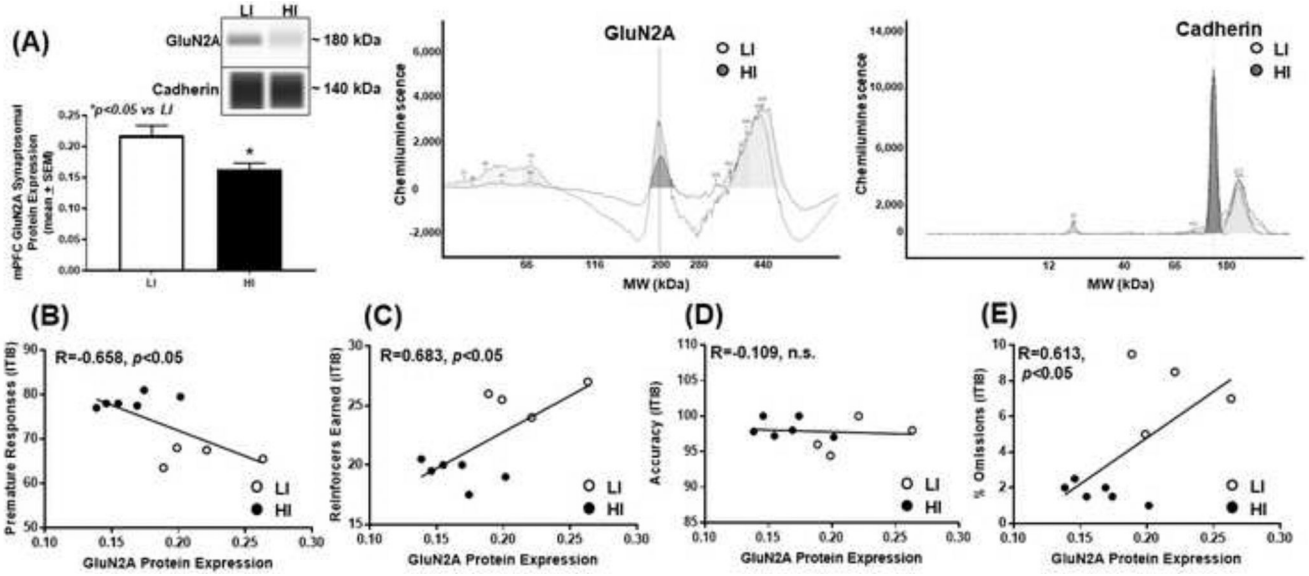

Figure 3. High trait motor impulsivity corresponds to lower GluN2A expression and correlates with additional measures from the 1-CSRT task.

(A) HI rats exhibit lower GluN2A versus LI rat (**p*<0.05 *vs.* LI*).* Virtual blot-like representative images generated directly from the chemiluminescent signal for the GluN2A and cadherin loading control were performed using crude synaptosomal protein from the mPFC (**inset**). The corresponding electropherograms with chemiluminescent signals for GluN2A and cadherin represents HI (dark grey) and LI (light grey) rats. Correlational analyses between **(B)** premature responses (R=−0.658; *p*<0.05), **(C)** reinforcers earned (R=0.683; *p*<0.05), **(D)** accuracy (R=−0.109; n.s.) and **(E)** percent omissions (R=0.613; *p*<0.05) and GluN2A protein expression.

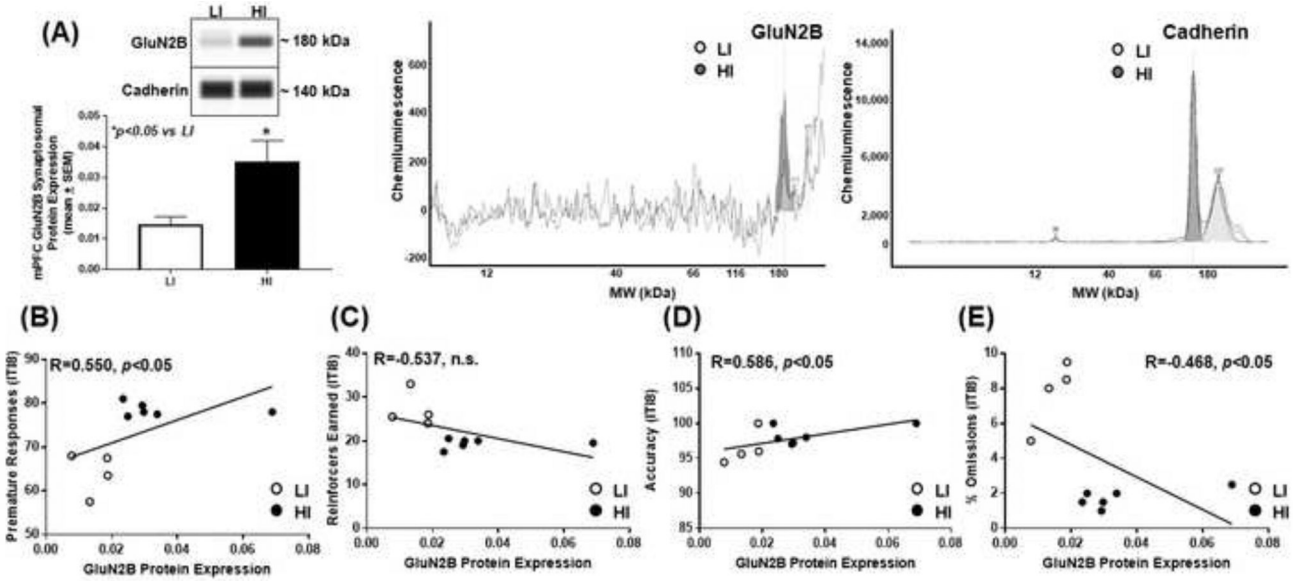

Figure 4. High trait motor impulsivity corresponds to higher GluN2B expression and correlates with additional measures from the 1-CSRT task.

(A) HI rats exhibit higher GluN2B versus LI rat (**p*<0.05 *vs.* LI*).* Virtual blot-like representative images generated directly from the chemiluminescent signal for the GluN2B and cadherin loading control were performed using crude synaptosomal protein from the mPFC (**inset**). The corresponding electropherograms with chemiluminescent signals for GluN2B and cadherin represents HI (dark grey) and LI (light grey) rats. Correlational analyses between **(B)** premature responses (R=0.550; *p*<0.05), **(C)** reinforcers earned (R= −0.537; n.s.), **(D)** accuracy (R=0.586; *p*<0.05) and **(E)** percent omissions (R=−0.468; n.s.) and GluN2B protein expression.

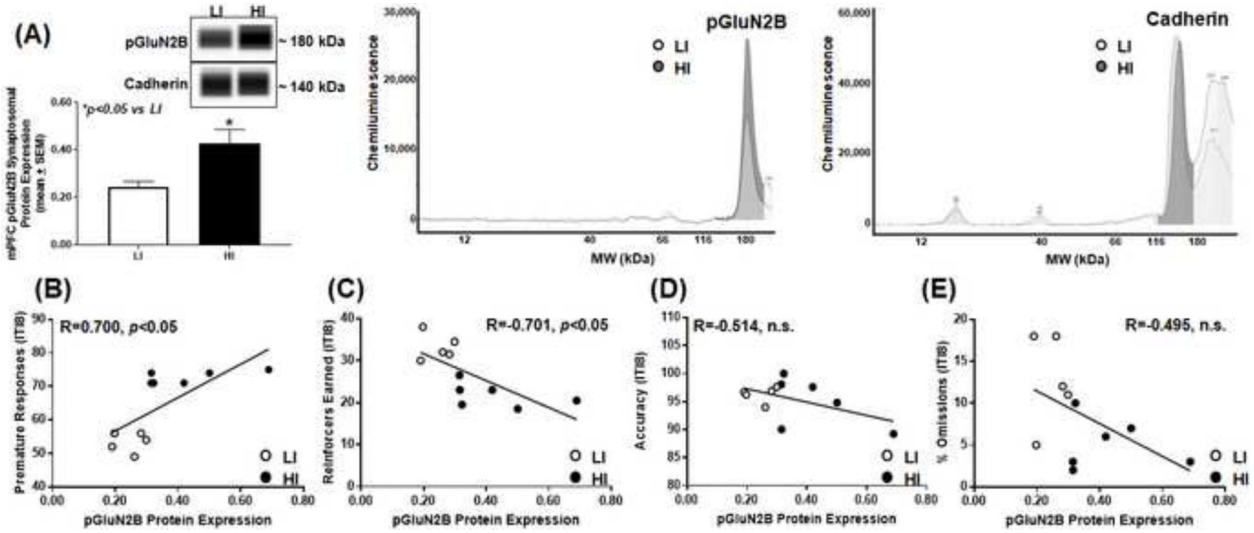

Figure 5. High trait motor impulsivity corresponds to higher pGluN2B expression and correlates with additional measures from the 1-CSRT task.

(**A**) HI rats exhibit higher pGluN2B versus LI rat (**p*<0.05 *vs.* LI*).* Virtual blot-like representative images generated directly from the chemiluminescent signal for the pGluN2B and cadherin loading control were performed using crude synaptosomal protein from the mPFC (**inset**). The corresponding electropherograms with chemiluminescent signals for pGluN2B and cadherin represents HI (dark grey) and LI (light grey) rats. Correlational analyses between **(B)** premature responses (R=0.700; *p*<0.05), **(C)** reinforcers earned (R= −0.701; *p*<0.05), **(D)** accuracy (R=−0.514; n.s.) and **(E)** percent omissions (R=−0.495; n.s.) and GluN2B protein expression.

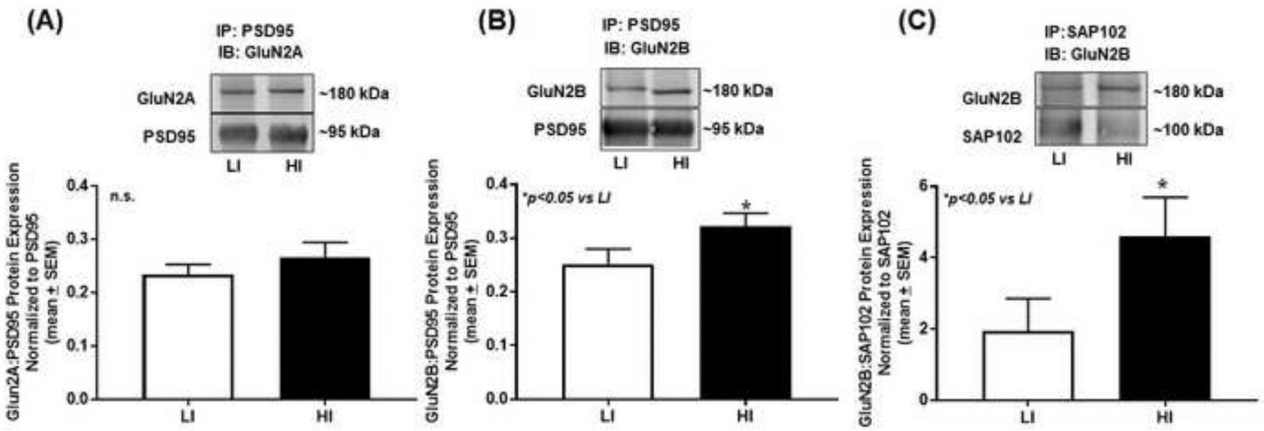

Figure 6. High trait motor impulsivity associates with GluN2B synaptic trafficking and stabilization.

(A) Immunoprecipitation (IP) for PSD95 followed by immunoblot (IB) for GluN2A yielded approximately equal association between PSD95 and GlunN2A (n.s.). **(B)** IP for PSD95 followed by IB for GluN2B revealed increased protein association between PSD95 and GluN2B in HI versus LI rats (*p<0.05 *vs.* LI). **(C)** IP for SAP102 and IB for GluN2B demonstrated that SAP102 associates with GluN2B to a higher extent in HI versus LI rats (*p<0.05 *vs.* LI). The insets are representative immunoblot bands. Arbitrary units (A.U.) of densitometry are presented.

Biochem Pharmacol. Author manuscript; available in PMC 2020 October 01.

Table 1.

Comparison of HI and LI identification across cohorts of outbred Sprague-Dawley rats

	LI (n=8–15/cohort)				
	Cohort 1 (mean ± SEM)	Cohort 2 (mean ± SEM)	Cohort 3 (mean ± SEM)	Cohort 4 (mean ± SEM)	Cohort 5 (mean ± SEM)
Premature Responses ($F_{4,57}$ = 6.153, p<0.05)	59.5 ± 1.9	54.7 ± 1.5	54.1 ± 0.9	50.2 ± 1.5	51.5 ± 0.8
Reinforcers Earned ($F_{4,57}$ =1.566, n.s.)	28.4 ± 1.3	31.8 ± 1.3	32.2 ± 1.4	33.3 ± 1.8	34.8 ± 2.0
Accuracy ($F_{4,57}$ = 0.889, n.s.)	96.4 ± 0.7	97.1 ± 1.0	96.0 ± 0.7	94.9 ± 1.2	96.6 ± 0.6
% Omissions ($F_{4,57}$ = 0.472, n.s.)	10.8 ± 1.5	12.7 ± 2.3	12.7 ± 1.4	14.6 ± 1.3	12.7 ± 2.5
Latency to Respond ($F_{4,57}$ = 1.66, n.s.)	1.5 ± 0.1	2.4 ± 0.6	2.3 ± 0.3	1.7 ± 0.1	1.7 ± 0.1
Time to Finish Session ($F_{4,57}$ = 1.07, n.s.)	1188.5 ± 18.3	1223.5 ± 24.2	1211.1 ± 12.0	1223.7 ± 11.5	1187.5 ± 18.0
	HI (n=9–15/cohort)				
	Cohort 1 (mean ± SEM)	Cohort 2 (mean ± SEM)	Cohort 3 (mean ± SEM)	Cohort 4 (mean ± SEM)	Cohort 5 (mean ± SEM)
Premature Responses ($F_{4,58}$ = 25.40, p<0.05)	80.1 ± 0.8*	76.0 ± 1.0*	72.2 ± 0.8*	67.2 ± 1.1*	69.4 ± 0.9*
Reinforcers Earned ($F_{4,58}$ = 15.78, p<0.05)	17.4 ± 0.8*	19.8 ± 0.9*	21.3 ± 0.9*	25.6 ± 0.9*	26.5 ± 1.0*
Accuracy ($F_{4,58}$ = 0.832, n.s.)	98.5 ± 0.9*	97.2 ± 0.8	95.7 ± 1.2	97.0 ± 0.7	96.6 ± 1.0
% Omissions ($F_{4,58}$ = 6.287, p<0.05)	2.1 ± 0.5*	3.1 ± 0.4*	5.8 ± 0.9*	6.7 ± 0.8*	4.1 ± 0.7*
Latency to Respond ($F_{4,58}$ = 2.28, n.s.)	1.6 ± 0.1	1.9 ± 0.2	2.4 ± 0.3	1.7 ± 0.1	1.9 ± 0.2
Time to Finish Session ($F_{4,58}$ = 5.69, p<0.05)	1077.0 ± 6.7*	1104.4 ± 15.1*	1138.2 ± 9.9*	1136.0 ± 6.6*	1129.6 ± 7.9*

HI and LI rats stratified on ITI8 challenge session.

*p<0.05 vs. LI within each respective cohort (Student's t-test); across cohorts an ordinary one-way ANOVA was employed for each output parameter of the 1-CSRT task. Latency to respond and time to finish are reported in seconds.